

Numerical Modeling of Internal Flow Aerodynamics

Part 1: Steady State Computations

Jean-François Guéry
 SNPE Propulsion
 Centre de Recherche du Bouchet
 F-91710 Vert-le-Petit
 FRANCE

NOTATIONS

E	total energy per unit of mass (J/kg)	T_f	propellant flame temperature (K)
F	convective flux vector in the x direction	u	velocity component in the x-longitudinal direction (m/s)
G	convective flux vector in the y direction	u_v	axial mean velocity (m/s)
H	convective flux vector in the z direction	v	velocity component in the y-lateral direction (m/s)
S	source term vector	v_{inj}	wall injection velocity (m/s)
k	turbulent kinetic energy	w	velocity component in the w-lateral direction (m/s)
\dot{m}_w	mass flow rate per injecting surface unit (kg/m ²)	x,y,z	co-ordinate system (m)
P	pressure (Pa)	ε	turbulent dissipation rate
P'	fluctuating pressure (Pa)	κ	thermal conductivity (W/mK)
Q	conservative variables vector of Navier-Stokes equations	μ	dynamic viscosity (kg/ms)
q_m	total mass flow rate (kg/s)	ρ	density (kg/m ³)
r_b	burning rate (mm/s)	ρ_s	propellant density (kg/m ³)
T	temperature of the flow (K)		

Dimensionless Parameter

Re_c	axial Reynolds number: $\rho u_v D_c / \mu$, where D_c is a characteristic diameter of the SRM
Re_s	wall injection Reynolds number: $\rho v_w D_c / \mu$
γ	isentropic exponent, equal to the specific heat ratio for a perfect gas

INTRODUCTION [1]

Internal ballistics in a SRM can be solved with various ways and for various objectives [2]. The motor design engineer wants to predict or understand the burning characteristics and the global performances of the motor, seek the efficiency of thermal insulation and nozzle design, check the reliability of ignition and motor design for the life cycle of the motor, take into account variability induced by manufacturing processes, etc.

Paper presented at the RTO/VKI Special Course on "Internal Aerodynamics in Solid Rocket Propulsion", held in Rhode-Saint-Genèse, Belgium, 27-31 May 2002, and published in RTO-EN-023.

Report Documentation Page				Form Approved OMB No. 0704-0188	
Public reporting burden for the collection of information is estimated to average 1 hour per response, including the time for reviewing instructions, searching existing data sources, gathering and maintaining the data needed, and completing and reviewing the collection of information. Send comments regarding this burden estimate or any other aspect of this collection of information, including suggestions for reducing this burden, to Washington Headquarters Services, Directorate for Information Operations and Reports, 1215 Jefferson Davis Highway, Suite 1204, Arlington VA 22202-4302. Respondents should be aware that notwithstanding any other provision of law, no person shall be subject to a penalty for failing to comply with a collection of information if it does not display a currently valid OMB control number.					
1. REPORT DATE 00 JAN 2004		2. REPORT TYPE N/A		3. DATES COVERED -	
4. TITLE AND SUBTITLE Numerical Modeling of Internal Flow Aerodynamics Part 1: Steady State Computations				5a. CONTRACT NUMBER	
				5b. GRANT NUMBER	
				5c. PROGRAM ELEMENT NUMBER	
6. AUTHOR(S)				5d. PROJECT NUMBER	
				5e. TASK NUMBER	
				5f. WORK UNIT NUMBER	
7. PERFORMING ORGANIZATION NAME(S) AND ADDRESS(ES) SNPE Propulsion Centre de Recherche du Bouchet F-91710 Vert-le-Petit FRANCE				8. PERFORMING ORGANIZATION REPORT NUMBER	
9. SPONSORING/MONITORING AGENCY NAME(S) AND ADDRESS(ES)				10. SPONSOR/MONITOR'S ACRONYM(S)	
				11. SPONSOR/MONITOR'S REPORT NUMBER(S)	
12. DISTRIBUTION/AVAILABILITY STATEMENT Approved for public release, distribution unlimited					
13. SUPPLEMENTARY NOTES See also ADM001656., The original document contains color images.					
14. ABSTRACT					
15. SUBJECT TERMS					
16. SECURITY CLASSIFICATION OF:			17. LIMITATION OF ABSTRACT UU	18. NUMBER OF PAGES 16	19a. NAME OF RESPONSIBLE PERSON
a. REPORT unclassified	b. ABSTRACT unclassified	c. THIS PAGE unclassified			

Different ways can be followed to reach the same goal. The reasons why a project manager uses numerical simulations are multiple. In the predictive mode, the aim is to design the system which fulfils the specifications at the lowest development cost (by minimizing the number of prototypes and tests). In the explanatory mode, the desire is to explain an observed and unknown phenomenon that happened during the development phase of a program.

For solid rocket motors, the objectives of internal flow computations are to predict the global performance and reliability of the rocket, avoid, minimize or master undesired behaviors (like thrust oscillations, erosive burning), take into account flow/grain and casing interactions (mechanical and thermal loads), etc.

The internal aerodynamics inside a solid rocket motor can be modeled with increasing degrees of complexity from the simplest global equations to a full 3D numerical simulations. An AGARD Lecture Series has already been organized on the Design Methods in Solid Rocket Motors [3]. The objective of this special course is not to duplicate the materials developed in AGARD-LS-150. We will focus on multidimensional simulations of internal flows.

Example of objectives and constraints:

- assessment of stability
- prediction of performances
- prediction of reliability
- prediction of variability, for instance thrust imbalance (important when using simultaneously more than one identical motor)

Conception:

- choose the right propellant for the application, and design the initial geometry of the solid propellant charge that will deliver, with surface regression, the required time history of the gas flow
- assess reliability of the designed motor (mechanical loads, ignition, casting process and raw materials variability, thrust oscillations, ...)

Challenges of numerical modeling:

- two-phase reacting flow (aluminized propellants)
- gas in a wide range of temperatures
- multi-species and turbulence
- two or three dimensional geometry
- moving boundaries
- fluid/structure coupling, with heterogeneous surface combustion
- steady and unsteady compressible flows, with all range of Mach number

The impact of numerical modeling in designing motors of new generation had a recent increase due to mainly three causes:

- large progress of computer power (hardware) and in computational fluid dynamics (software) in the last decades
- objective of cost reduction (mainly in the development phase of a new motor)
- new objectives of performance and reliability

An improved prediction reduces the number of qualifying fires, and for large and expensive motors, this is of prime importance.

This lecture series will be divided in two special courses. The first one presents the general models for solving internal steady state aerodynamic in solid rocket motors, the second one focus on pressure and thrust oscillations modeling.

GENERAL EQUATION FOR AERODYNAMICS

At a starting point, the general equations describing fluid flows inside a solid rocket motor begins with the Navier-Stokes equation. We remind them as an introduction.

The general form of the conservation equations for a three dimensional viscous flow can be written in the following form:

$$\frac{\partial Q}{\partial t} + \frac{\partial F}{\partial x} + \frac{\partial G}{\partial y} + \frac{\partial H}{\partial z} = S$$

where:

$$Q = \begin{bmatrix} \rho \\ \rho u \\ \rho v \\ \rho w \\ \rho E \end{bmatrix}$$

$$F = \begin{bmatrix} \rho u \\ \rho u^2 + P - \sigma_{xx} \\ \rho uv - \sigma_{xy} \\ \rho uw - \sigma_{xz} \\ (\rho E + P)u - u\sigma_{xx} - v\sigma_{xy} - w\sigma_{xz} - \kappa \frac{\partial T}{\partial x} \end{bmatrix}$$

$$G = \begin{bmatrix} \rho v \\ \rho uv - \sigma_{xy} \\ \rho v^2 + P - \sigma_{yy} \\ \rho vw - \sigma_{yz} \\ (\rho E + P)v - u\sigma_{xy} - v\sigma_{yy} - w\sigma_{yz} - \kappa \frac{\partial T}{\partial y} \end{bmatrix}$$

$$H = \begin{bmatrix} \rho w \\ \rho u w - \sigma_{xz} \\ \rho v w - \sigma_{yz} \\ \rho w^2 + P - \sigma_{zz} \\ (\rho E + P)w - u\sigma_{xz} - v\sigma_{yz} - w\sigma_{zz} - \kappa \frac{\partial T}{\partial z} \end{bmatrix}$$

and S is the source term vector.

These equations must be solved with appropriate solvers and on appropriate grids.

Over the last twenty years, different grid technologies have been developed. Based on experience on finite difference schemes and for the sake of simplicity in software management, structured grids have been widely used. A structured grid is a grid where each component can be identified by two indices (i,j) in 2D and three indices (i,j,k) in 3D. Each index refers to a space dimension. Hence, the grid points are ordered, giving the name of “structured grid”. However, this technology was shown very precise and efficient for a simple geometry but limited for a complex geometry. Techniques of multiple structured domains overlapping have been developed, but with special difficulties for ensuring global conservation among the different domains and a good efficiency on distributed memory parallel computers.

For an unstructured flow solver, the computational domain is tessellated using a grid composed of simplices, which are quadrilaterals or triangles in two dimensions and generally tetrahedras, pyramids, pentagons, prisms and hexahedras in three dimensions. Unstructured grids provide flexibility for tessellating about complex geometry and for adapting to flow features, such as shocks and boundary layers.

On a given grid, one has the option of locating the variables at the cell centers or at the vertices of the grid, giving rise to cell-centered and cell-vertex schemes. Alternatively, it is possible to deal strictly with averages defined over volumes. This approach has certain advantages for higher order schemes. In the case of finite volume schemes, the governing equations are discretized. This allows discontinuities to be captured as part of the solution.

SOLID PROPULSION MODELS

General modern CFD codes for computing flows in solid rocket motors have the following features:

- solves the 2D axisymmetrical, plane and 3D Navier-Stokes equations for laminar or turbulent flows
- uses unstructured meshes for complex geometry treatment
- has the possibility for treating the chemical reactions of multi-species and the coupling between a gas phase and a condensed phase, inert or not, with specific models
- has moving mesh facilities
- incorporates specific solid propulsion models for the burning rate, from simple laws (regression rate) to several coupling (ignition, erosive burning, unsteady combustion) as well as solid propellant grain coupling (mechanical, surface-burnback).

COMBUSTION AND EROSIVE BURNING

Erosive burning is a phenomenon commonly experienced in a solid propellant rocket motor, represented by an increase of the local propellant burning rate due to high velocity combustion gas flow across the burning surface. Most propellants have a minimum cross-flow velocity below which erosive burning is not observed, referred to as the “threshold velocity”.

The erosive burning mechanism is believed to be due to the:

- increase in gas-to-solid heat feedback caused by the increase in transport coefficients
- turbulence-enhanced mixing and chemical reaction of the oxidizer and fuel rich gases pyrolyzed for composite propellants

Steady combustion is a complex mechanism including chemical and physical effects (nature and details of energetic materials and additives, particle size distribution, operating conditions: pressure, initial temperature, radiation, ...). For erosive burning, the cross-flow velocity (parallel to the solid propellant burning surface) constitutes an additional operating condition of extreme importance.

Several theoretical approaches have been reported, which can be grouped in five categories, following Kuo and coworkers [4]:

- 1) phenomenological heat transfer theories
- 2) modification of the propellant combustion mechanism
- 3) integral boundary layer analysis
- 4) chemically reacting turbulent boundary layer analysis
- 5) others

We focus on models 1 and 4. Models in the category 1 will have an interest for engineering design problems while models in the category 4, relying on more fundamental viewpoint, are thought to be more precise and thus more appropriate for being incorporated in complex CFD codes.

Phenomenological Heat Transfer Theories

Most of these models are based on or derived from Lenoir & Robillard [5] approach, giving the general expression for the burning rate in the form:

$$r_b = aP^n + \frac{\alpha G^g}{f(D_h)} e^{-\frac{\beta \rho_s r_b}{G}}$$

where α , β and g are three constants, G is the mass flux through the port, and D_h is the hydraulic diameter. The expression $f(D_h)$ can include scale effects. In the original form, $f(D_h)=D_h^{0.2}$, $\beta=53$ is found to be independent of the propellant type, and $g=0.8$ (based on Chilton-Coburn correlation for evaluating the convective heat transfer coefficient).

This approach is well suited for 1D analysis.

Chemically Reacting Turbulent Boundary Layer Analysis

These models are well suited to aerothermochemical analysis of erosive burning of composite propellants, and many authors have contributed (King [6], Beddini, Kuo, and people from ONERA). We will focus on ONERA approach [7,8] used at SNPE.

The turbulent flow is solved in a high Reynolds approach and the propellant surface is treated as a wall zone. In this region, Couette equations are solved, from the propellant surface to the first integration point of the flow in the port. The temperature gradient in the flame is then computed, leading to the heat flux to the surface. A flame height criterion is used, assuming that the combustion between oxidizing and fuel gases is limited by the diffusion (valid for medium and large AP sizes). In the erosive regime, the solution of the Couette flow is coupled with the flame height criterion, including the turbulent contribution. This coupled system is solved in an iterative way, until the velocity and temperature profiles match the values of the first integration point in the flow. At convergence, the erosive burning rate is immediately obtained.

Since it is driven by viscous effects, the erosive burning in a SRM will be sensitive to the scale of the motor.

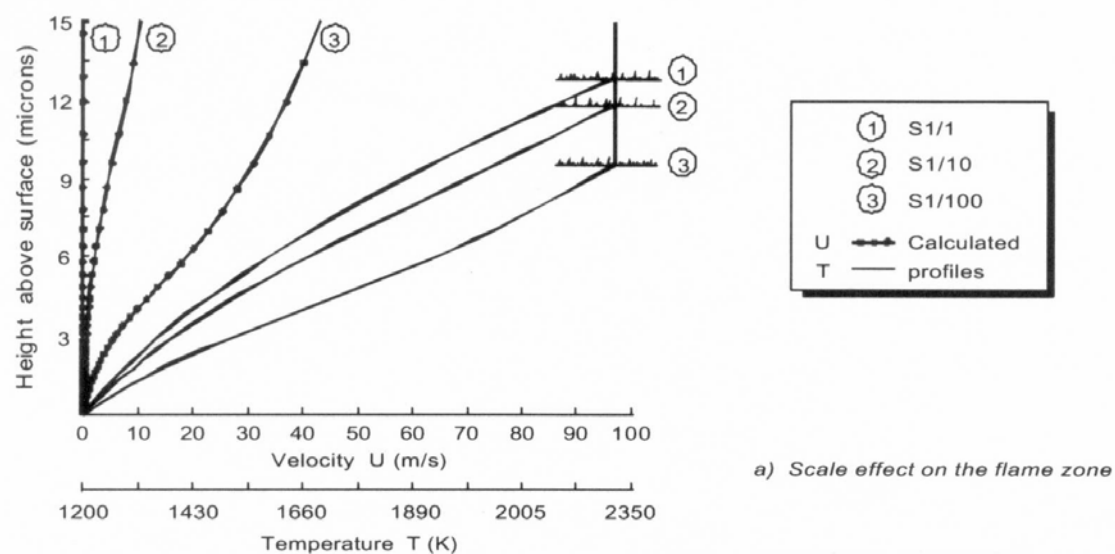


Figure 1: Flame Zone Computed by the ONERA Model at Different Scales (1, 1/10 and 1/100).

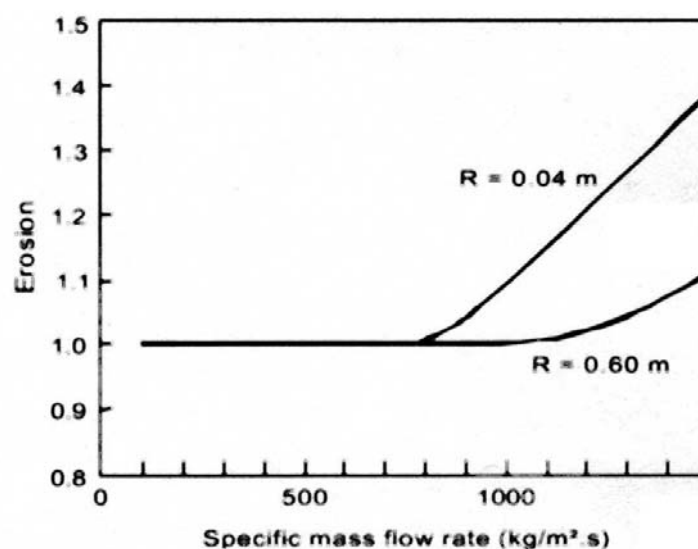


Figure 2: Erosive Behavior as a Function of the Motor Scale (ONERA Model).

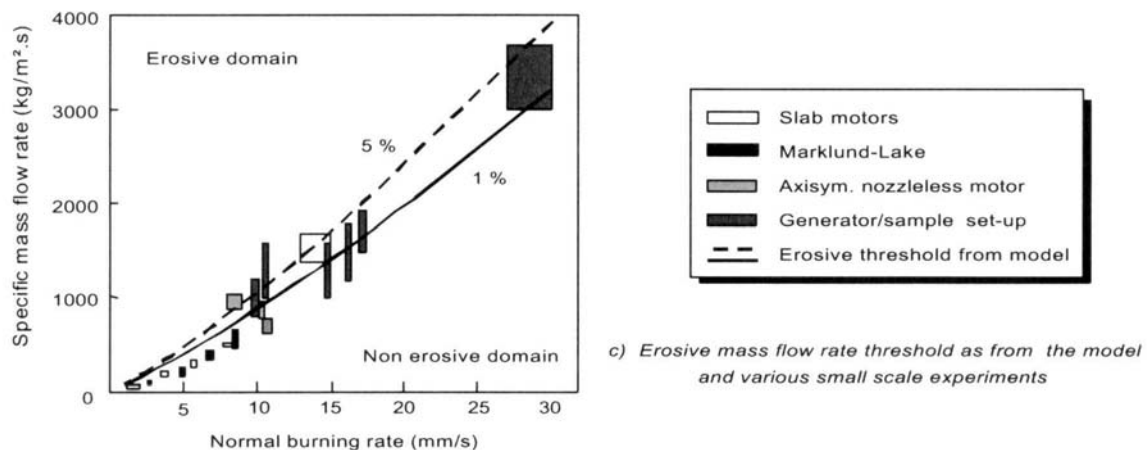


Figure 3: Erosive Threshold in Various Configurations (ONERA Model).

TURBULENCE

Turbulence modeling in the port becomes necessary for the evaluation of heat transfer and/or diffusion related phenomena (erosive burning, heat flux over thermal inhibitors and material decomposition, ...).

Cold flow experiments with wall injection have shown that this kind of flow have a delayed turbulent transition, as illustrated on Figure 4. The important parameter is the injection Reynolds number (defined with injection velocity at the blowing surface and port radius). For injection Reynolds number above 50, the transition from a laminar to a turbulent flow is delayed.

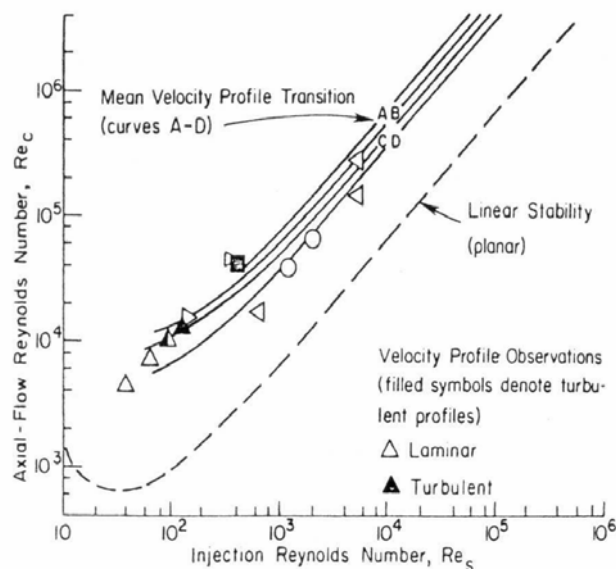


Figure 4: Laminar / Turbulent Transition as a Function of the Injection Reynolds Number.

The difficulty in simulating turbulence in a SRM comes from the fact that the transition is always inside the port, since the velocity at the head-end is equal to zero. So, turbulence modeling must compute correctly the transition. A schematic view of laminar-turbulence interaction is given in Figure 5.

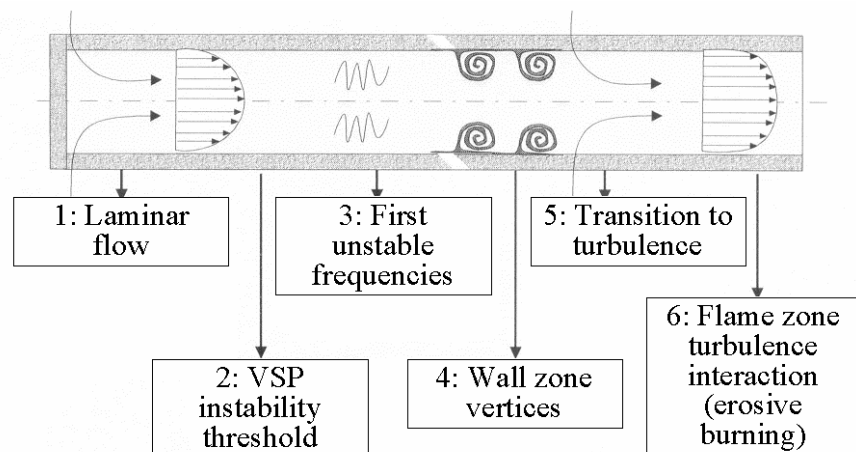


Figure 5: Schematic View of Laminar-Turbulence Transition in a SRM.

Usually, classical turbulence models are used for internal flows in SRM. As in the usual treatment of turbulence, the velocity field u and pressure P are decomposed into mean \underline{u} , \underline{P} and fluctuating u' , P' parts with Favre's average for compressible flows.

Two-equation models, like the $k-\varepsilon$ model, solves transport equations for the turbulent kinetic energy k and the dissipation rate ε . Source terms (S) are accounted for modeling turbulence creation and dissipation. The eddy viscosity is expressed as a function of k^2/ε and the Boussinesq hypothesis is used for computing the turbulent stresses.

Classical $k-\varepsilon$ turbulence models are isotropic, and this hypothesis is very restrictive for flows in SRM. Anisotropic turbulence models, like Algebraic Stress Models (ASM) are an efficient way for improving turbulence modeling without a dramatic CPU increase.

Flow turbulence modeling must always be associated with a consistent injection modeling. As the difficulty is in predicting turbulence transition, the flow features must be well described at injection. This can be done by solving the boundary zone with Couette or Prandtl equations, as for the erosive burning modeling, or with approximated laws [9].

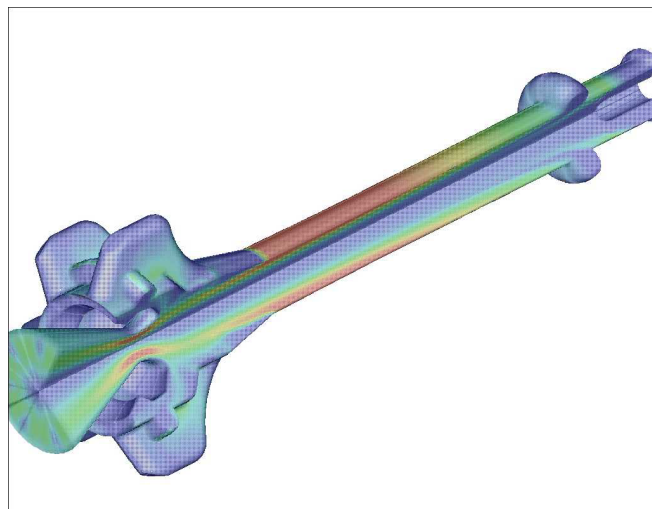


Figure 6: Computation of Turbulence Level in a Finocyl SRM (SNPE).

TWO-PHASE FLOW EFFECTS

Many solid rocket motors use aluminized propellants in order to improve their performances. The aluminum combustion produce a condensed phase (aluminum oxide), and therefore a two-phase flow in the rocket chamber.

An important consequence of the presence of this liquid phase is two-phase losses, and in the case of large segmented motors with a submerged nozzle, slag accumulation, which may have several consequences on specific impulse, thermal insulation behavior and thrust vectoring.

Continuous efforts have been done, for many years, in the USA, in Russia and in France, in order to develop numerical models able to predict accurately losses and the slag formation.

More details can be found in Salita special course [10].

An eulerian or a lagrangian description can be used for the condensed phase.

In the eulerian description, the condensed phase is assumed to be a continuous medium, and the conservation equation are derived from integrals of conservative quantities (mass, momentum and energy) on control volumes. The following vectors are added to the gas phase vector in the previous form of the conservation equation [11]:

$$Q_p = \begin{bmatrix} \rho_p \\ \rho_p u_p \\ \rho_p v_p \\ \rho_p w_p \\ \rho_p E_p \end{bmatrix}$$

$$F_p = \begin{bmatrix} \rho_p u_p \\ \rho_p u_p^2 \\ \rho_p u_p v_p \\ \rho_p u_p w_p \\ (\rho_p E_p) u_p \end{bmatrix} \quad G_p = \begin{bmatrix} \rho_p v_p \\ \rho_p u_p v_p \\ \rho_p v_p^2 \\ \rho_p v_p w_p \\ (\rho_p E_p) v_p \end{bmatrix} \quad H_p = \begin{bmatrix} \rho_p w_p \\ \rho_p u_p w_p \\ \rho_p v_p w_p \\ \rho_p w_p^2 \\ (\rho_p E_p) w_p \end{bmatrix}$$

and the source term S account for gas-condensed phase interactions. In these expressions, subscript p refers to the particulate phase. The volume fraction of the dispersed phase is noted α_p and is supposed to be small (for being neglected in the gas phase equations). Apparent condensed phase density, ρ_p , is equal to $\rho_p = \alpha_p \rho_p$ where ρ_p is the condensed phase true density.

The eulerian method is well suited for particles with a fixed diameter. Generally, aluminum oxide particle show a bi or trimodal distribution after aluminum combustion (resulting from smoke, nominal aluminum residues and agglomerated aluminum residues). According to its small size and relaxation time, the smoke can be treated with the equivalent gas. Generally, one or two classes (diameter) or particles are used in the computation. Even if it is possible in the eulerian form, for coupling the particle velocity field with turbulence or taking into account complex phenomena such as coalescence or break-up, the lagrangian method is more appropriate.

In the lagrangian method, group of particles are emitted from the propellant surface and are explicitly followed in the flow. It allows more complex physics to be taken into account since it approaches the “discrete form” of the condensed phase, but the lagrangian method is CPU time consuming for a correct treatment of the flow (approaching the apparent particle density in the flow).

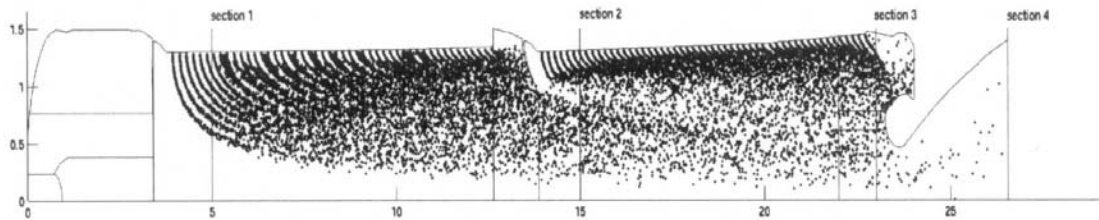


Figure 7: Lagrangian Computation of the Two-Phase Flow in Ariane 5 SRM [13].

Two-Phase Losses

These losses are created by the non equilibrium between gas and condensed phase from the chamber to the throat. In the converging part of the nozzle, the flow is accelerated and the condensed phase is accelerated by the flow. An important parameter will be the ratio of condensed phase relaxation time over the transit time in the nozzle. If we note R this ratio:

- for small R , the particles are in equilibrium with the gas, they are accelerated and give their thermal energy (temperature) to the gas, contributing to the impulse;
- for large R , particles will be in non-equilibrium with the gas, and an impulse deficit will be created.

Additional phenomena to take into account are particles break-up and phase changes.

Investigation of the Slag Formation [12]

Slag is generated, either when aluminum oxide droplets impinge on some portion of the back-face of the nozzle, or when they are captured in the recirculation zone behind the submerged nozzle. This phenomenon generally produces a slag pool in the aft end of the motor and an aluminum oxide liquid film on some part of the nozzle wall.

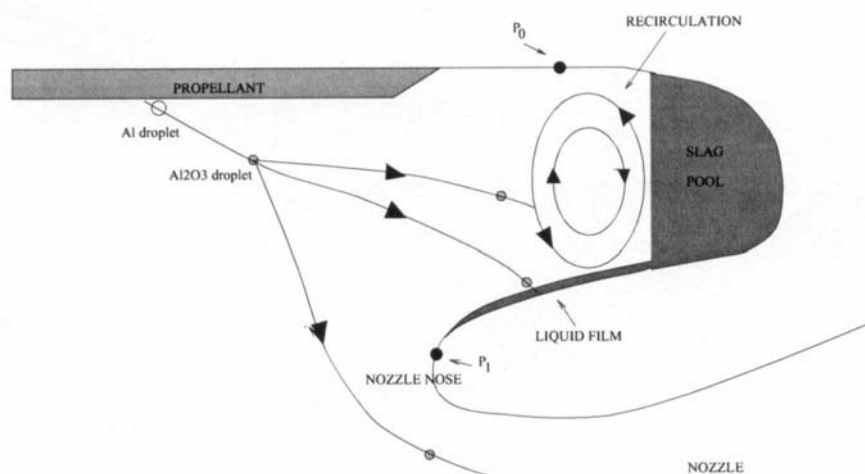


Figure 8: Schematic View of Main Phenomena Leading to Slag Formation.

Different strategies can be applied to the slag formation investigation: a fully coupled numerical computation, or a two step, uncoupled, computation.

The principle of a two-step uncoupled calculation can be summarized as follows [13]:

- 1) The steady state of the gas flowfield must be calculated with an appropriate turbulence model; the presence of the liquid phase must be taken into account by assuming that the two phases are at equilibrium everywhere in the booster (same temperature, same velocity and constant density ratio deduced from the propellant composition), using the equivalent gas (see chapter on thermochemistry).
- 2) The condensed phase consists only of aluminum oxide droplets, ejected directly from the propellant surface; when the combustion zone is small compared to motor geometry, no combustion model need to be used; the droplet size distributions, used in the simulations, must follow the experimental distribution, measured with a quench bomb.
- 3) If the motion of the droplets is simulated by a Lagrangian method, all the trajectories are calculated on the steady gas flowfield and a stochastic model can be used to take into account the influence of the turbulence field on the droplet dispersion.
- 4) The total slag rate can be calculated by summing the weights of all the droplets which impinged the nozzle back-face in the stagnation zone or which are trapped in the recirculation zone in the aft end of the motor.

If the motor is unstable, a coupling may exist between vortex-shedding and particles behavior in the flow. In that particular case, an unsteady computation of this coupling is necessary [14].



Figure 9: Computation of the Coupling between Vortex-Shedding and Two-Phase Flow in an Unstable Segmented Solid Rocket Motor (Particles Volume Fraction).

THERMOCHEMISTRY

Since the flame zone in SRM is very small compared to motor length, we can consider that the injected gas from the burning surface are the final combustion products.

Generally, their thermochemical properties are computed from equilibrium computer codes, most of them based on the original Gordon and Mc Bride CEC71 code [15]. Since classical computations are done with constant thermodynamic properties, the validity of assumptions made for computing them must be checked. Classically, two thermodynamic parameters are taken: the frozen heat capacity and γ in the motor. As an illustration, the evolution of the frozen heat capacity of a composite solid propellant is given as a function of the Mach number in a SRM (from the chamber to the throat) in Figure 10.

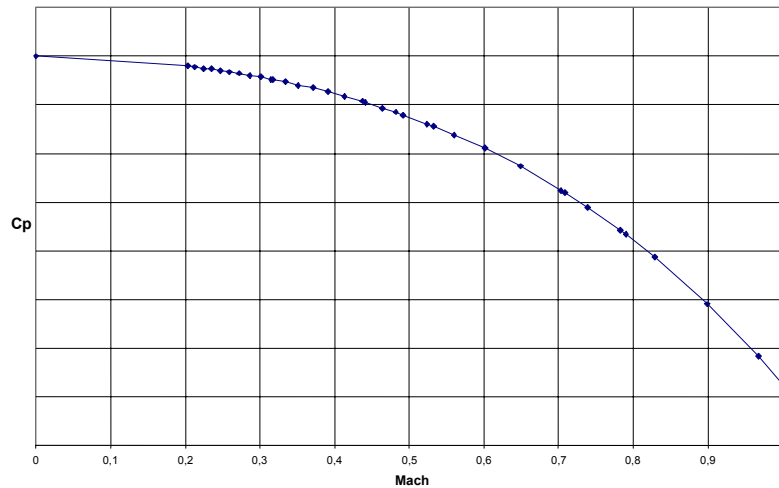


Figure 10: Example of the Evolution of the Heat Capacity with the Mach Number in the Convergent Part of a Nozzle.

Another approximation can be made by writing the combination of Saint-Venant and enthalpy conservation equation:

$$T_f = T(1 + \frac{\gamma - 1}{2} M^2)$$

and using this equation at the throat ($M=1$) for computing an approximated γ with the value of the temperature at the throat computed by the thermodynamical code.

This equation also shows that temperature and velocity or pressure and density are correlated in a SRM, and that temperature and pressure are independant.

The other thermodynamic parameter, for instance the specific heat capacity, can be adjusted for giving the correct characteristic velocity c^* , hence the correct pressure.

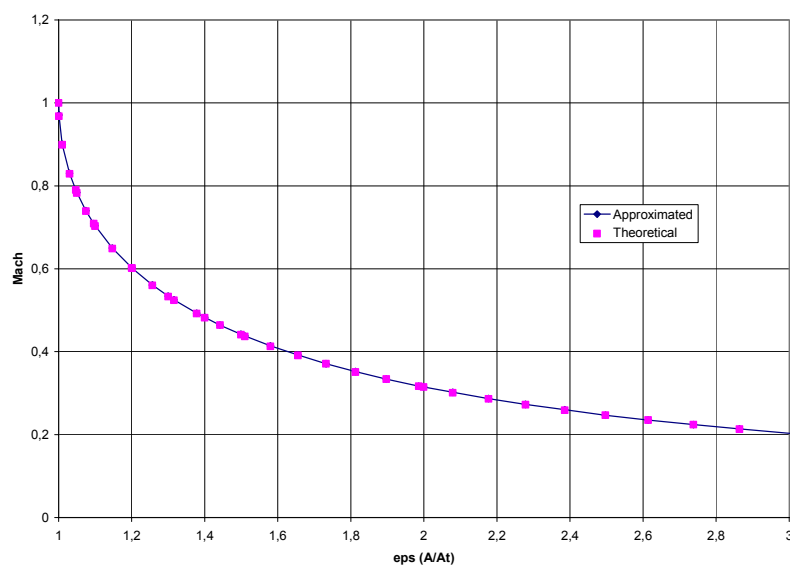


Figure 11: Comparison of Theoretical and Approximated Pressure in a Nozzle.

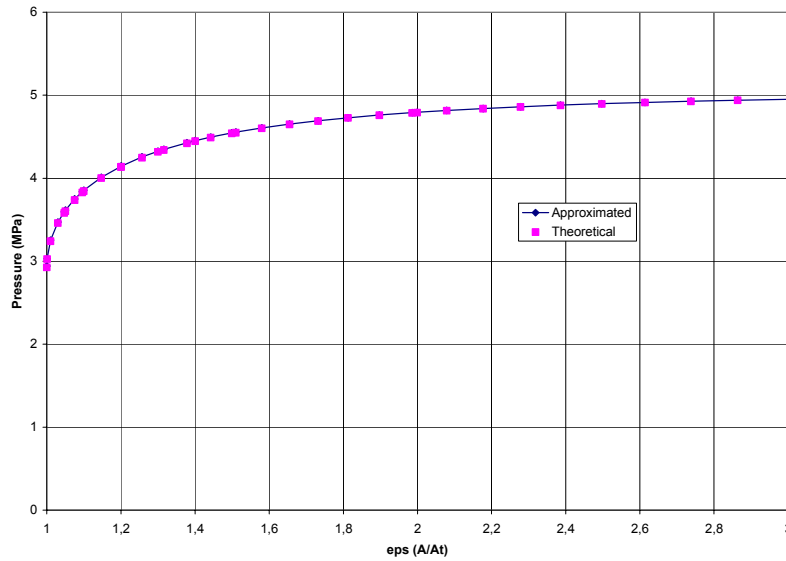


Figure 12: Comparison of Theoretical and Approximated Pressure in a Nozzle.

For a two-phase flow approximation, the following relations must be written for the heat capacity and specific heat ratio:

$$c_p^g = (1 + C_m)c_p - C_m c_p^p$$

$$\gamma^g = \frac{1}{1 - (1 + C_m) \frac{c_p}{c_p^g} \frac{\gamma - 1}{\gamma}}$$

where the subscripts ^g and ^p are for the gaz and particulate phase in the two-phase approximation, and C_m is the condensed phase / gas phase mass flow rate ratio.

RECENT DEVELOPMENTS: FLUID-STRUCTURE INTERACTION [16]

Fully coupled solution of fluid flows with structural interactions is called fluid-structure interaction. The range of its applications is important in many engineering disciplines [17]. Some current applications are pressure waves in a piping system, sound waves traveling through fluid-solid media, biomedical problems such as blood flow in a diseased artery or coupled instabilities in power systems. Computer-aided techniques for design optimization have been much promoted over the past decades and have subsequently reached a high level of sophistication within many single disciplines such as fluid or structural mechanics. However, because of complexity and computational cost issues, most often the coupling effects are neglected. For example, in aerodynamics optimization, the structure is assumed to be rigid. Another reason for separate treatment is the schismatic split-up of engineering disciplines, which makes it difficult for one person to have in-depth knowledge on all of these. With the computer power increasing and the advent of parallel processing, research on fluid-structure interaction in the field of numerical aeroelastic simulations has received growing interest in the last ten years.

In fluid-structure interactions, the combined effects of inertial, elastic and aerodynamic forces impact the movement of the fluid and solid boundaries. The fluid movement exerts aerodynamic forces on the structure that reacts and in turn forces the flow to evolve at the interface with an interface velocity. This produces the coupling effect and suitable computational strategies need to be developed. The problem

of the motion of the fluid-structure interface that occurs in coupled aeroelastic problems is generally addressed by solving the fluid equations on moving dynamic meshes with an Arbitrary Lagrangian Eulerian formulation.

Fluid structure computation has applications in solid propellant grain mechanical design and unsteady simulations.

Main Features of the Modeling

Mathematical models of coupled problems are usually coupled partial differential equations in space and time. Often, different discretization techniques are used on the different physical components. The most difficult part of handling numerically the fluid-structure coupling arises from the fact that the structural equations are usually formulated with lagrangian coordinates while the flow equations are expressed using eulerian coordinates. These physically heterogeneous system components are computationally treated as isolated entities that are separately advanced in time. Interaction effects are viewed as forcing effects that are communicated between the individual components.

Arbitrary Lagrangian Eulerian Formulation

The ALE formulation consists in solving the conservation equation on a moving grid. Since if the grid is fixed, the method is called eulerian, and the method is called lagrangian for grid points having the material velocity, the ALE formulation is a generalization.

Numerical fluxes must be computed correctly through the moving faces [17].

In order to solve the problem, the computational mesh has to be moved or deformed during the time integration of the fluid. A common technique to deform a mesh is the spring analogy. The force exerted by the nodes j which are connected to the node i is mathematically expressed by:

$$\sum_j \kappa_{ij} (\vec{x}_j - \vec{x}_i)$$

where κ_{ij} is the stiffness of the spring between nodes i and j . At equilibrium state, the force at every node i has to be zero. After regrouping the terms, the iterative equation to be solved yields:

$$\vec{x}_i^{k+1} = \sum_j \kappa_{ij} \vec{x}_j^k / \sum_j \kappa_{ij}$$

Structural Model

The structural model can go from a simple reduction of stiffness, mass and damping matrices of the finite element mechanical model on the fluid boundary to the full resolution with a non linear structural mechanics code.

Fluid-Structure Coupling Algorithm

The coupling algorithm is performed in a staggered way. Structure and fluid are integrated on the same time scale (given by the fluid time step required by the fluid solver) although the characteristic scales for the structural system and for the fluid flow may be very different.

The fluid and structure equations are coupled by imposing that at the boundary, the structure stress tensor is in equilibrium with the fluid pressure and that wall boundary condition occurs on the fluid-structure interface. It implies that the forces and energies exchanged at the fluid-structure interface are balanced. Moreover, mesh and structure motions are also coupled by continuity conditions on the interface.

A complete cycle takes place as follows:

- 1) The fluid transmits to the structure a pressure profile obtained at time n to evaluate the pressure forces exerted by the fluid F^n .
- 2) The structure model determines the displacements q^{n+1} .
- 3) This structure configuration is transmitted to the fluid model.
- 4) Fluid variables W are then advanced at time $n + 1$.
- 5) Back to step 1.

The position of the structure at time $n + 1$ is advanced with pressure force input F^n defined from a fluid pressure profile and then the flow state vector W^{n+1} is computed from the mesh configurations $x^n = q^n$ to $x^{n+1} = q^{n+1}$. The position of the dynamic fluid mesh does not lag behind that of the surface of the structure.

With no damping matrix $[D]$, the structural energy expresses as:

$$E_s = \frac{1}{2} {}^t q [K] q + \frac{1}{2} {}^t \dot{q} [M] \dot{q} + {}^t q F_0$$

and its variation during a time step is $\Delta E_s = E_s^{n+1} - E_s^n = ({}^t q^{n+1} - {}^t q^n) F^n$ deriving from the structural time integrator. On the other hand, the transferred energy through an element of the fluid-structure interface can be written as $\Delta E_f = ({}^t x^{n+1} - {}^t x^n) P$ where P is the nodal fluid force whose expression depends on the fluid pressure values used by the flow solver to compute the fluxes across the fluid-structure interface. The force and energy exchanged between the fluid and the structure at their interface must be opposed. To ensure these principles, a procedure enforcing momentum or energy conservation is used at the interface in step 4. To do it, fluid pressure involved in the boundary flux is re-adjusted. The simplest way is to estimate P and F^n with the mean value of the gas pressure available at the beginning of cycle.

CONCLUDING REMARKS

In this lecture, an overview of general problems and models used in CFD code for SRM steady interior flows has been made. The second paper will focus on unsteady phenomena.

REFERENCES

- [1] A. Davenas et al, "Solid Rocket Propulsion Technology", Pergamond Press, 1993.
- [2] F. Godfroy and G. Delannoy, "La Modélisation des Ecoulements dans les systèmes propulsifs et les dispositifs pyrotechniques", Revue Scientifique de la Défense, 1997-3, pp. 63-74.
- [3] AGARD-LS-150, "Design Methods in Solid Rocket Motors".

- [4] K.K. Kuo and M. Summerfield et al, “Fundamentals of Solid Propellant Combustion”, AIAA PAAS Vol. 90.
- [5] J.M. Lenoir and G. Robillard, “A Method to Predict the Effects of Erosive Burning in Rocket Motors”, 6th Symposium on Combustion, 1957.
- [6] M.K. King, “Erosive Burning of Solid Propellants”, Combustion of Solid Propellants, AGARD-LS-180, 1991.
- [7] J.C. Godon, J. Duterque and G. Lengellé, “Solid Propellant Erosive Burning”, Journal of Propulsion and Power, 8(4), pp. 741-747, 1992.
- [8] J.C. Godon, J. Duterque and G. Lengellé, “Erosive Burning in Solid Propellant Motors”, Journal of Propulsion and Power, 9(6), pp. 806-811, 1993.
- [9] I. Tseng, I-Shih and V. Yang, “Combustion of a Double-Base Homogeneous Propellant in a Solid Rocket Motor”, Combustion and Flame, Vol. 96-4, 1994.
- [10] M. Salita, “Two-Phase Flows in Rocket Motors”, RTO-AVT-VKI Special Course, Internal Aerodynamics in Solid Rocket Propulsion, May 2002.
- [11] V. Morfouace and P.Y. Tissier, “Two-Phase Flow Analysis of Instabilities Driven by Vortex-Shedding in Solid Rocket Motors”, AIAA-95-2733, July 1995.
- [12] J. Dupays, Y. Fabignon, P. Villedieu, G. Lavergne and J.L. Estivalezes, “Some Aspects of Two-Phase Flows in Solid Propellant Rocket Motors”, in Solid Propellant Chemistry, Combustion and Motor Interior Ballistics, Progress in Astronautics and Aeronautics, Vol. 185, 2000.
- [13] P. Villedieu, Y. Fabignon, J.F. Guéry, F. Godfroy, P. Le Helley, J. Hylkema, L. Jacques and G. Lavergne, “Slag Accumulation in Large Segmented Solid Rocket Motors with a Submerged Nozzle”, Space Solid Propulsion Conference, Rome, November 2000.
- [14] F. Godfroy and J.F. Guéry, “Unsteady Eulerian Two-Phase Flow Analysis of Solid-Propellant Rocket Motor Slag”, AIAA-97-2859, July 1997.
- [15] S. Gordon and B.J. McBride, “Computer Program for Calculation of Complex Chemical Equilibrium Compositions, Rocket Performance, Incident and Reflected Shocks and Chapman-Jouguet Detonation”, NASA-Lewis Research Center, SP-273, 1971.
- [16] P. Della Pieta et al, “Numerical Simulations of Some Fluid-Structure Interaction Phenomena Found in Solid Rocket Motors”, paper submitted for publication to the Journal of Propulsion and Power.
- [17] A. Dervieux et al, “Fluid-Structure Interaction”, Revue Européenne des Eléments Finis, Vol. 9, October 2000.